Natural diamond formation by self-redox of ferromagnesian carbonate

Ming Chen[a,b,1], Jinfu Shu[c], Xiande Xie[b,d], Dayong Tan[b,d], and Ho-kwang Mao[c,e,1]

[a]State Key Laboratory of Isotope Geochemistry, Guangzhou Institute of Geochemistry, Chinese Academy of Sciences, 510640 Guangzhou, China; [b]Key Laboratory of Mineralogy and Metallogeny, Guangzhou Institute of Geochemistry, Chinese Academy of Sciences, 510640 Guangzhou, China; [c]Center for High Pressure Science and Technology Advanced Research, 201203 Shanghai, China; [d]Guangdong Provincial Key Laboratory of Mineral Physics and Materials, Guangzhou Institute of Geochemistry, Chinese Academy of Sciences, 510640 Guangzhou, China; and [e]Geophysical Laboratory, Carnegie Institution of Washington, Washington, DC 20015

Contributed by Ho-kwang Mao, January 31, 2018 (sent for review November 28, 2017; reviewed by Eglantine Boulard and Alexander V. Soldatov)

Formation of natural diamonds requires the reduction of carbon to its bare elemental form, and pressures (*P*) greater than 5 GPa to cross the graphite–diamond transition boundary. In a study of shocked ferromagnesian carbonate at the Xiuyan impact crater, we found that the impact pressure–temperature (*P-T*) of 25–45 GPa and 800–900 °C were sufficient to decompose ankerite $Ca(Fe^{2+},Mg)(CO_3)_2$ to form diamond in the absence of another reductant. The carbonate self-reduced to diamond by concurrent oxidation of Fe^{2+} to Fe^{3+} to form a high-*P* polymorph of magnesioferrite, $MgFe^{3+}{}_2O_4$. Discovery of the subsolidus carbonate self-reduction mechanism indicates that diamonds could be ubiquitously present as a dominant host for carbon in the Earth's lower mantle.

diamond | self-redox | ferromagnesium carbonate | shock-metamorphism | lower mantle

Natural diamonds are a rare metastable mineral on Earth's surface; they form under high pressure–temperature (*P-T*) conditions that are generated either from static compressions at depths greater than ∼150 km (1, 2) or from dynamic compressions during meteoritic impacts on shallow crustal rocks (3, 4). These two types of diamonds bring unique, complementary information about the environment and processes of their formation and preservation. The xenocrystic diamonds from depth encapsulate inclusions during formation, providing some of the most valuable, direct samples of Earth's deep mantle (5). These deep-Earth diamonds and their mineral inclusions, however, come from very selective regions and form by a range of processes, often involving fluids and melts, and are not therefore a representative sample of the interior. Their inclusions are also small selective samples of what could be trapped inside the diamonds during diamond growth; they do not reveal the full petrology and mineralogy surrounding the diamonds. The strong, inert diamond capsule protects the chemistry of its inclusions, but does not retain the original total pressure (6). Thus, high-*P* phases in the inclusion are seldom preserved (7), but often convert to low-*P* polymorphs and/or exsolve to mixed-mineral assemblages during the long, slow journey of exhumation. Intensive research on deep Earth diamonds over the past half-century has provided extraordinarily rich information on the formation of lithospheric diamonds from 150- to 240-km depth (∼5–8 GPa), which consist of >95% of observed natural diamonds. Solid carbonates are stable in the relatively oxidized lithosphere where diamond formation is predominantly from special C–O–H fluids (5). The investigated sublithospheric, or superdeep, diamonds and their inclusions provide valuable information for the formation of diamonds from depths beneath the lithosphere (8–10).

On the other hand, diamonds produced by meteoritic impact have the advantage of preserving in situ the diamonds together with coexisting high *P-T* minerals, as well as the original petrological and mineralogical settings. The coverage of meteoritic impacts is global and random, but the targets are limited to crustal rocks exposed on the surface. Like a natural experiment, the rapid quenching rate provides the optimal condition for retaining the high *P-T* minerals. In fact, most high-*P* minerals stable in the deep Earth, such as the first known high-*P* silica, coesite (11), and the most abundant mantle mineral, bridgmanite (12), were originally discovered in terrestrial impact craters and shocked meteorites, respectively. Impact diamonds provide valuable, complementary information for understanding the origin of deep-mantle diamonds.

Impact diamonds cover a very wide range of initial compositions and *P-T* conditions. For instance, previously reported impact diamonds from the Popigai crater formed from isomorphic transitions of elemental carbon graphite (4), whereas diamonds from the Ries crater crystallized from very high-*T* melts or by chemical vapor deposit (3). By studying the petrography of diamonds in a shocked Fe^{2+}-bearing carbonate at the Xiuyan crater, we discovered important evidence for diamond formation directly from ferromagnesite carbonate, which by extension could be dominant in the deep mantle. We found that diamonds were formed from ankerite via a subsolidus self-oxidation–reduction reaction under shock-induced high *P-T* conditions. Carbonate in ankerite, $Ca(Fe^{2+},Mg)(CO_3)_2$, decomposed and reduced to diamond by simultaneous oxidation of its ferrous iron to ferric iron, resulting in the formation of magnesioferrite and a high-*P* polymorph of magnesioferrite, $MgFe^{3+}{}_2O_4$. This mechanism implies that in the lower mantle with the presence of magnesium and ferrous iron, carbonates could decompose to diamonds, and diamond could be a very abundant form of carbon.

Significance

The presence of extra reducer was thought to be essential for producing natural diamonds from reduction of carbonates. The present study of the Xiuyan meteoritic crater, however, finds natural diamond formation via a subsolidus self-redox of a ferromagnesian carbonate during shock compression to 25–45 GPa and 800–900 °C without melting, fluid, and another reductant. The ability of carbonate to produce diamond by itself implies that diamond would be a very common mineral in the lower mantle where the carbonates are abundant and pressures and temperatures are sufficiently high.

Author contributions: M.C. and H.-k.M. designed research; M.C., J.S., X.X., D.T., and H.-k.M. performed research; M.C., J.S., X.X., and D.T. analyzed data; and M.C. and H.-k.M. wrote the paper.

Reviewers: E.B., Institut de Minralogie, de Physique des Matriaux et de Cosmochimie; and A.V.S., Luleå University of Technology.

The authors declare no conflict of interest.

[1]To whom correspondence may be addressed. Email: mchen@gig.ac.cn or mao@gl.ciw.edu.

This article contains supporting information online at www.pnas.org/lookup/suppl/doi:10.1073/pnas.1720619115/-/DCSupplemental.

Published online February 26, 2018.

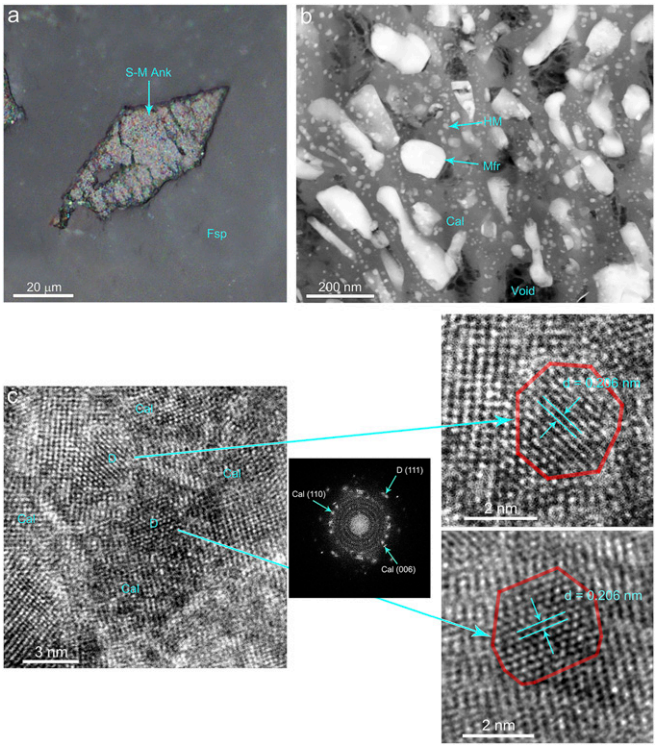

Fig. 1. Mineral phases in shock-metamorphic ankerite. (*A*) Shock-metamorphic ankerite (S-M Ank) enclosed in feldspar (Fsp) in shock-metamorphic gneiss; plane-polarized reflected light. (*B*) An STEM image shows high-*P* polymorph of magnesioferrite (HM) and magnesioferrite (Mfr), calcite (Cal), and voids in the shock-metamorphic ankerite. HM occurs as nanocrystals of 2–30 nm in size, whereas magnesioferrite occurs as crystallites up to 300 nm in size. (*C*) High-resolution TEM image of nanodiamonds (D) enclosed in calcite (Cal) together with the Fourier transform diagram of the image area. Local high-magnification images show two nanocrystals of diamond within the red frames. The interplanar distance of the (111) lattice planes of diamond are 0.206 nm.

Sample Observation and Characterization

The hypervelocity impact of asteroids and comets on the Earth's surface can cause high *P* and high *T* in target rocks and lead to shock metamorphism of rocks and minerals, generating high *P-T* phases like coesite (11) and diamond (4) at Earth's surface. We investigated the shock effects on ferromagnesian carbonate by meteorite impact in the Xiuyan crater, China. The crater is 1.8 km in diameter and located on the Proterozoic metamorphic complex composed of gneiss, amphibolite, granulite, and marble. The gneiss contains about 5% ankerite. Other mineral components of the gneiss include quartz, feldspar, and hornblende, as well as the accessory minerals rutile, zircon, and magnetite. Our study focused on the moderately shock-metamorphosed gneiss rock fragments in an impact breccia recovered from drill cores of the crater. The gneiss samples have an estimated peak shock *P* of 35–45 GPa, and show no shock-induced melting. Quartz and feldspar in the gneiss partially transformed into diaplectic glasses (13, 14), rutile partially transformed into its high-*P* polymorph TiO_2-II (13), and zircon partially transformed into reidite (14).

Ankerite in the gneiss was shock-metamorphosed and decomposed. We can see the coexistence of shock-metamorphic ankerite, TiO_2-II, and reidite on the samples of gneiss (Fig. S1). Pseudomorphs of the original ankerite crystals (Fig. 1*A*) are clearly visible. On the thin sections, the shock-metamorphic ankerite appears dark blown or opaque under polarized transmitted light, and with a pearly luster under plane-polarized reflected light. The bulk chemical composition of ankerite as determined by electron microprobe analysis is $Ca(Fe_{0.59}Mg_{0.33}Ca_{0.07}Mn_{0.01})^{2+}(CO_3)_2$ (Table S1). Microscopic analyses using Raman spectroscopy, synchrotron X-ray diffraction, scanning/transmission electron microscope (STEM), and transmission electron microscope (TEM) show that ankerite decomposed into a multiphase mixture composed of diamond, magnesioferrite, a high-*P* postspinel phase of magnesioferrite, and calcite (Fig. 1*B*). Magnesioferrite and high-*P* magnesioferrite occur as granular and elongate crystallites 20–300 nm in size and both have the same chemical composition with a formula of $(Mg_{0.62}Fe_{0.35}Mn_{0.03})^{2+}Fe^{3+}{}_2O_4$ (Table S2), i.e., $Fe^{3+}/\sum Fe = 0.85$. Diamond occurs as nanocrystallites of 2–5 nm in size (Fig. 1*C*). Calcite occurs as polycrystalline aggregates with the individual crystal size ranging from 5 to 100 nm. Some nanoscale voids are also observed in the shock-metamorphic ankerite. Based on the phase distributions on the thin sections (Fig. 1*B*) and the relative intensity of X-ray diffraction peaks (see Fig. 3), the shock-metamorphic ankerite contains around 20% magnesioferrite, 8% high-*P* magnesioferrite, and 3% diamond. The relatively low contents of high-*P* magnesioferrite and diamond correspond to a short duration of high pressure caused by meteorite impact.

High-*P* magnesioferrite, magnesioferrite, calcite, and diamond have been identified in the shock-metamorphic ankerite by Raman spectroscopy (Fig. 2 and Fig. S2). The Raman spectrum of magnsesioferrite is characterized by a strong band at 686 cm^{-1} and weak bands at 554, 478, 328, and 210 cm^{-1}, in agreement with typical Raman features of magnesioferrite (15). The intense band at 686 cm^{-1} can be assigned to the A_{1g} oscillation mode of a spinel structure (16). The Raman spectrum of high-*P* magnesioferrite displays a strong band at ~602 cm^{-1} (Fig. S2), which is similar to the postspinel phase of $FeCr_2O_4$ (17). The Raman measurements of magnesioferrite at pressure up to 51.6 GPa and room temperature found that magnesioferrite becomes amorphized at above 27.7 GPa (18). In our sample, we obtained three typical Raman spectra which characterize a change of peak intensity at 686 cm^{-1} or at 602 cm^{-1} (Fig. S2). The peaks' intensity evolution in the spectra from Fig. S2 *A–C* provides a convincing argument that the peak intensity evolution of 602 and 686 cm^{-1} from Fig. S2 *A–C* corresponds to the relative contents between magnesioferrite and high-*P* magnesioferrite at the analyzed spots. The band at 602 cm^{-1} is attributed to the high-*P* polymorph of magnesioferrite, whereas the band at 686 cm^{-1} is assigned to magnesioferrite. The Raman signal of calcite shows a strong band at 1,086 cm^{-1} and a weak band at 279 cm^{-1}, in good agreement with the typical Raman

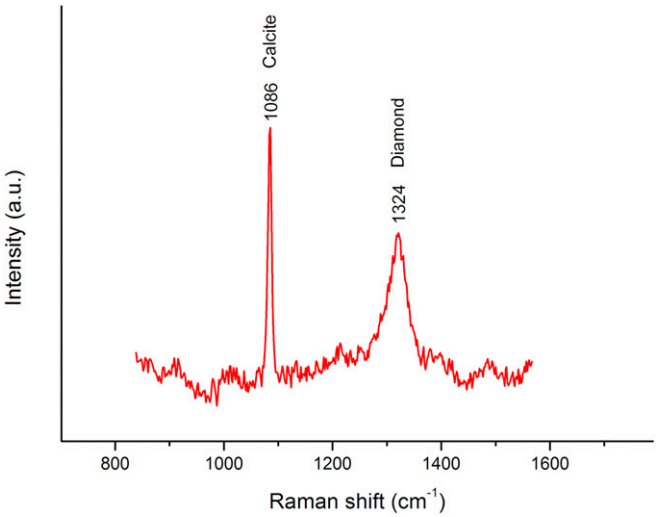

Fig. 2. Raman spectrum (laser 638 nm) of diamond from shock-metamorphic ankerite. The broadened peak around 1,324 cm^{-1} is attributed to ultratiny crystallites of diamond. The peak at 1,086 is assigned to calcite.

feature of calcite (19). The Raman signal of diamond is characterized by a broadened band around 1,324 cm^{-1} with a full width at half maximum (FWHM) of 39 cm^{-1} (Fig. 2). The relatively lower wavenumber than that of normal diamond (1,331 cm^{-1}) corresponds to the effect of ultrafine nanodiamond undergoing a low-frequency shift accompanied by peak broadening (20, 21). According to the correlation among frequencies, FWHM of Raman band at 1,324 cm^{-1}, and crystallite size (20), the nanocrystal size of diamond can be estimated as 3–5 nm, in agreement with our TEM observation.

After Raman spectroscopic analyses, the same grain of shock-metamorphic ankerite has been used for X-ray diffraction analyses. The crystal structures of high-*P* magnesioferrite, magnesioferrite, calcite, and diamond in the shock-metamorphic ankerite have been investigated in situ on thin sections by synchrotron X-ray microdiffraction (Fig. S3). More than 20 diffraction lines have been collected from high-*P* magnesioferrite (Table S3), which can be indexed to an orthorhombic $CaFe_2O_4$-type postspinel structure with the space group *Pnma*, and the orthorhombic unit-cell parameters of high-*P* magnesioferrite are a = 8.907(1) Å, b = 9.937(8) Å, c = 2.981(1) Å. Two clear diffraction peaks including (111) and (220) from diamond are well indexed (Fig. 3). High-resolution TEM images together with the Fourier transform diagram of the image area identify the nanodiamonds with an interplanar distance of 2.06 Å which can be referred to the (111) lattice planes of diamond (Fig. 1*C*). Magnesioferrite and calcite are also well indexed from the X-ray diffraction pattern (Table S4).

Discussions and Geological Implications

Ankerite in the target gneiss of the Xiuyan crater had apparently decomposed during the impact event. The decomposition of ankerite is thus characterized by the chemical reaction:

$$\begin{aligned}&6\mathrm{Ca}\left(\mathrm{Fe}_{2/3}\mathrm{Mg}_{1/3}\right)^{2+}(\mathrm{CO}_3)_2(\text{ankerite})\\&\rightarrow 6\mathrm{CaCO}_3+2\mathrm{MgFe}_2^{3+}\mathrm{O}_4(\text{high-}P\text{ magnesioferrite})\\&+\mathrm{C}(\text{diamond})+5\mathrm{CO}_2.\end{aligned}\qquad[1]$$

Along with oxidation of Fe^{2+} to Fe^{3+}, carbon in ankerite had been reduced to diamond. $CaCO_3$ adopts a high-*P* format *P* above 8 GPa (22).

Shockwave propagation in rocks results in a rapid rise in *P*, *T*, and density, and leads to phase transformations in natural samples similar to laboratory experiments (23). The *P* and *T* of the Xiuyan crater can be estimated based on the known experimental conditions of the observed high-*P* minerals. Quartz in the gneiss sample has been mostly transformed into diaplectic glasses (13, 14). The impact-caused transformation of quartz to diaplectic glass constrains a relatively low shock *T* of 300–900 °C at a peak shock *P* of 35–45 GPa (24). The shock-metamorphic gneiss in the Xiuyan crater contains abundant high-*P* phases of TiO_2-II and reidite formed by rapid solid-state transformation (13, 14), thus constraining the *T* to >800 °C (25). The shock *T*, therefore, can be estimated as 800–900 °C. The stability fields of TiO_2-II (26) and reidite (27) limit the *P* to above 15 GPa. No previous experimental study is known for the present high-*P* magnesioferrite composition that is close to 2:1 solid solution of magnesioferrite:magnetite. The spinel–postspinel transition boundaries for the endmembers magnesioferrite at 25 GPa (28) and magnetite at 23.6 GPa (29) are within the above *P-T* constraints. Overall, the conditions for diamond formation are constrained to a *T* of 800–900 °C, and *P* of 25–45 GPa, which reaches lower mantle pressures. Under this *P-T* condition, CO_2 remains a solid phase (30) like all other minerals in Eq. **1**.

Although formation of diamonds from subsolidus decomposition of carbonates without iron metal or sulfide as external reductants has not been reported in nature, such reactions are a logical extension of a number of previous studies. $CaCO_3$ is an inactive component in Eq. **1**, so that we can focus on the ferromagnesian carbonate portion of the reaction.

$$6\left(\mathrm{Fe}_{2/3}\mathrm{Mg}_{1/3}\right)^{2+}\mathrm{CO}_3\rightarrow 2\mathrm{MgFe}_2^{3+}\mathrm{O}_4+\mathrm{C}(\text{diamond})+5\mathrm{CO}_2.\qquad[2]$$

Low-*P* decomposition of Fe^{2+}-bearing carbonate (siderite) to graphite and magnetite has been reported from terrestrial metamorphic rocks (31). Recent experiments over a wide range of high *P* (40–105 GPa) and high *T* (1,200–3,300 °C) demonstrate that the chemical reaction among $Fe^{2+}O$, $(Mg,Fe^{2+})O$, and CO_2 can lead to the formation of diamond and Fe^{3+}-bearing phases (32, 33). Thus, under the lower-mantle *P*, ferrous iron in carbonates can act as a reductant similar to metallic iron to reduce CO_2 for the production of elemental carbon in the form of diamond.

Intensive research on deep-Earth diamonds over the past half-century has provided evidence that most observed lithospheric

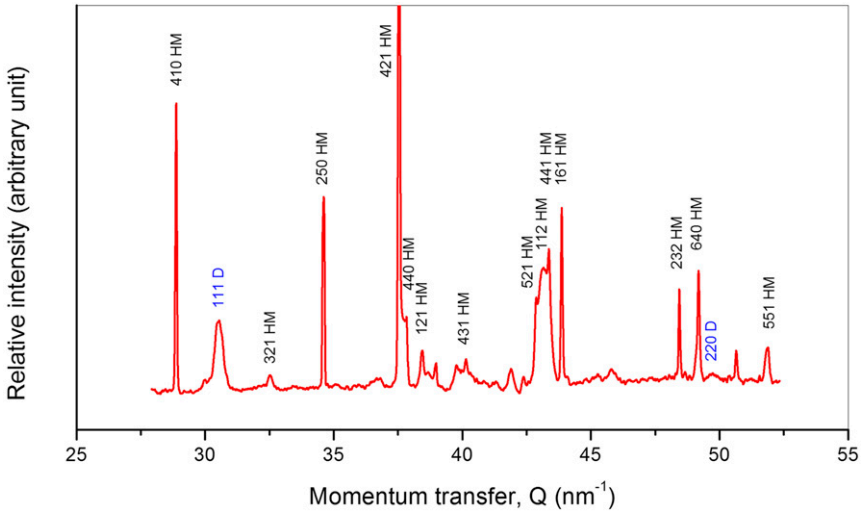

Fig. 3. X-ray diffraction pattern of shock-metamorphic ankerite. Two diffraction lines were indexed to the (111) and (220) planes of diamond (D), respectively. Other diffraction lines are from high-*P* polymorph of magnesioferrite (HM).

diamonds are from a mobile carbon-bearing phase, commonly referred to as "C–O–H-bearing fluid or melt" (5). While these fluids give diamond the remarkable ability to track carbon mobility and reveal mineralogy and redox state in the deep lithospheric mantle, they represent a very small portion of the total carbon flux and inventory (34). What about the carbon outside these fluids? Most diamonds (~95%) derive from the lithosphere at depths of 150–250 km (~5–8 GPa) where solid carbonates are stable at relatively oxidized conditions, and diamond formation requires C–O–H fluids. At greater depth the mantle becomes more reducing, however, and diamonds should be able to form with an appropriate carbon source and reduction mechanism.

Our knowledge of the superdeep diamonds and carbonates from depth below the lithosphere comes from a small subset (<5%) of extensively investigated samples (8–10). Redox freezing and melting of ferrous carbonate has been proposed (35) and observed (36) for the formation of superdeep diamonds by simultaneous disproportionation of Fe^{2+} to Fe^{3+} plus metallic Fe^0. This self-redox mechanism is similar to the present observation of impact diamonds, except it involves the presence of metallic Fe and carbonated melts (10, 35), which only occurs in specific regions and may be a typical case of the predominantly solid lower mantle. The key question remains as, what is the predominant form of carbon and its associated minerals in the vast, solid deep lower mantle?

The Xiuyan crater provides a concrete natural example that at *P* equivalent to the lower mantle, diamonds can form by self-redox of ferromagnesian carbonates alone without melting and in the absence of metallic iron. Ferromagnesian carbonates are among the dominant carbonates in organic-rich oceanic sedimentary environments on the Earth, especially in the pre-1.8-Gy sedimentary sequences (37), and the generalized decomposition mechanism in Eq. **2** could be widespread in the lower mantle.

Moreover, ferromagnesian carbonates are chemical equivalent of ferromagnesian oxide plus CO_2, and diamonds can also form in the mantle by reactions between CO_2 and the dominant mantle oxide (Fe,Mg)O:

$$CO_2 + 6\left(Fe^{2+}_{2/3}Mg_{1/3}\right)O(\text{ferropericlase}) = C(\text{diamond}) + 2MgFe^{3+}_2O_4. \quad [3]$$

Formation of diamonds and ferric-bearing phases from reaction of CO_2 and ferropericlase has been observed in experiments equivalent to the lower-mantle conditions at 55–105 GPa (32). With the omnipresence of ferropericlase in the lower mantle, CO_2 produced from ferromagnesian carbonate by Eqs. **1** or **2** or from decomposition of iron-free carbonates could be reduced to diamonds with a byproduct of ferric-bearing high-*P* magnesioferrite. Consequently, diamond would be a common host of carbon in the lower mantle without the need of another reductant and regardless of solid or molten states.

Thomson et al. (10) suggested that carbonated oceanic crust subducted into the deep upper mantle and transition zone would melt due to a deep depression along the solidus, thus forming a barrier to carbonate subduction, and suggested that superdeep diamonds form due to redox freezing when carbonated melts react with the ambient mantle. The present diamond formation mechanism does not require melting nor metallic Fe, but indicates that in the reducing deep mantle, carbonate will self-reduce to form diamond. This further generalizes the carbonate barrier concept (10) to cover the entire lower-mantle *P-T* conditions where diamonds can be formed from ferromagnesian carbonate (Eq. **2**), and from CO_2 in the presence of ferropericlase (Eq. **3**).

Inclusions of ferropericlase are generally regarded as an index mineral for superdeep diamonds. If superdeep diamonds are formed from self-redox of ferromagnesian carbonate or reaction of CO_2 with ferropericlase, the key product would be a ferric iron compound. Indeed, magnesioferrite is often observed in recent reports of superdeep diamonds (38, 39). The present example indicates that the very high $Fe^{3+}/\sum Fe$ ratios of 0.67–1.0 in the magnetite to magnesioferrite series, respectively, reflect the spinel chemistry and do not infer the overall oxygen fugacity. Therefore, the ferropericlase-magnesioferrite are good indicators of the superdeep diamonds (38, 39).

In conclusion, the observation of Xiuyan impact diamonds and experiment results in recent literature provide valuable insights to deep carbon in the lower mantle. With the subsolidus self-reduction mechanism of superdeep diamond formation, another reductant and melting conditions are no longer required; the presence of ferromagnesian carbonates or CO_2 and ferropericlase is sufficient. This makes superdeep diamond very abundant in its natural habitat. Its scarcity is thus due to the difficulty of preservation through the journey to the surface.

Methods

The samples of gneiss from impact breccia of the Xiuyan crater were made into polished thin sections for physical and chemical analyses of minerals. Petrologic and mineralogical features as well as shock effects of minerals were firstly identified on thin sections by optical microscopy. Determination of mineral phases and structures was conducted by multiple microbeam analytical techniques (*SI Text*), including Raman spectroscopy, electron microprobe, synchrotron-radiation X-ray microdiffraction, focused ion beam (FIB) milling, and STEM. FIB milling was used to extract slices of sample for STEM and TEM analyses. Contamination of thin sections by diamond from polishing compound has been a longstanding problem in some previous studies. The fact that diamond is found in slices extracted and thinned by FIB techniques proves that it is diamond indigenous to the section and produced by the impact and would thus rule out any contamination by polishing compound. Chemical compositions of the mineral phases were obtained by using an electron microprobe and energy-dispersive X-ray spectrometry.

ACKNOWLEDGMENTS. We are very grateful to Steven B. Shirey and two reviewers for valuable comments and suggestions which greatly improve the quality of this paper. We thank Y. P. Yang from HPSTAR in Shanghai for FIB milling of TEM samples; and H. Y. Xian from GIGCAS in Guangzhou for TEM analysis, B. B. Yue (HPSTAR), F. Hong (HPSTAR), and N. Tamura (ALS) of Beamline 12.3.2 at the Advanced Light Source of the Lawrence Berkeley National Laboratory for synchrotron X-ray microdiffraction analysis. M.C. and D.T. were supported by the Strategic Priority Research Program (B) of the Chinese Academy of Sciences (XDB18010405), and the National Natural Science Foundation of China (41672032). H.-k.M. was supported by NSF Geophysics Grant EAR-1345112 and Geochemistry Grant EAR-1447438. This work was also partially supported by the National Natural Science Foundation of China (Grant U1530402).

1. Haggerty SE (1999) A diamond trilogy: Superplumes, supercontinents, and supernovae. *Science* 285:851–860.
2. Dobrzhinetskaya L, Wirth R, Green H (2014) Diamonds in Earth's oldest zircons from Jack Hills conglomerate, Australia, are contamination. *Earth Planet Sci Lett* 387:212–218.
3. Hough RM, et al. (1995) Diamond and silicon carbide in impact melt rock from the Ries impact crater. *Nature* 378:41–44.
4. Jones AP, et al. (2016) Structural characterization of natural diamond shocked to 60 GPa; implications for Earth and planetary systems. *Lithos* 265:214–221.
5. Shirey SB, et al. (2013) Diamonds and the geology of mantle carbon. *Rev Mineral Geochem* 75:355–421.
6. Sobolev NV, et al. (2000) Fossilized high pressure from the Earth's deep interior: The coesite-in-diamond barometer. *Proc Natl Acad Sci USA* 97:11875–11879.
7. McCammon C, Hutchison M, Harris J (1997) Ferric iron content of mineral inclusions in diamonds from Sao Luiz: A view into the lower mantle. *Science* 278:434–436.
8. Walter MJ, et al. (2011) Deep mantle cycling of oceanic crust: Evidence from diamonds and their mineral inclusions. *Science* 334:54–57.
9. Stagno V, Ojwang DO, McCammon CA, Frost DJ (2013) The oxidation state of the mantle and the extraction of carbon from Earth's interior. *Nature* 493:84–88.
10. Thomson AR, Walter MJ, Kohn SC, Brooker RA (2016) Slab melting as a barrier to deep carbon subduction. *Nature* 529:76–79.
11. Chao ECT, Shoemaker EM, Madsen BM (1960) First natural occurrence of coesite. *Science* 132:220–222.
12. Tschauner O, et al. (2014) Mineralogy. Discovery of bridgmanite, the most abundant mineral in Earth, in a shocked meteorite. *Science* 346:1100–1102.
13. Chen M, Gu X, Xie X, Yin F (2013) High-pressure polymorph of TiO_2-II from the Xiuyan crater of China. *Chin Sci Bull* 58:4655–4662.
14. Chen M, et al. (2013) Natural occurrence of reidite in the Xiuyan crater of China. *Meteorit Planet Sci* 48:796–805.

15. Winell S, Annersten H, Prakapenka V (2006) The high-pressure phase transformation and breakdown of $MgFe_2O_4$. *Am Mineral* 91:560–567.
16. D'Ippolito V, Andreozzi GB, Bersani D, Lottici PP (2015) Raman fingerprint of chromate, aluminate and ferrite spinels. *J Raman Spectrosc* 46:1255–1264.
17. Chen M, Shu J, Mao HK, Xie X, Hemley RJ (2003) Natural occurrence and synthesis of two new postspinel polymorphs of chromite. *Proc Natl Acad Sci USA* 100:14651–14654.
18. Wang Z, Lazor P, Saxena SK, O'Neill HSC (2002) High-pressure Raman spectroscopy of ferrite $MgFe_2O_4$. *Mater Res Bull* 37:1589–1602.
19. Sun J, Wu Z, Cheng H, Zhang Z, Frost RL (2014) A Raman spectroscopic comparison of calcite and dolomite. *Spectrochim Acta A Mol Biomol Spectrosc* 117:158–162.
20. Aleksenskiĭ AE, Baĭdakova MV, Vul AY, Davydo VY, Pevtsova YA (1997) Diamond graphite phase transition in ultradisperse-diamond clusters. *Phys Solid State* 39: 1007–1015.
21. Panda K, et al. (2012) Tribological properties of ultrananocrystalline diamond and diamond nanorod films. *Surf Coat Tech* 207:535–545.
22. Koch-Müller M, Jahn S, Birkholz N, Ritter E, Schade U (2016) Phase transitions in the system $CaCO_3$ at high P and T determined by in situ vibration spectroscopy in diamond anvil cell and first-principles simulations. *Physcs and Chemistry of Materals* 43: 545–561.
23. Sharp TG, DeCarli PS (2006) *Meteorites and the Early Solar System II*, eds Lauretta DS, McSween HYJ (Univ of Arizona Press, Tucson, AZ), pp 653–677.
24. Grieve RAF, Langenhorst F, Stöffler D (1996) Shock metamorphism of quartz in nature and experiment: II. Significance in geoscience. *Meteorit Planet Sci* 31:6–35.
25. Akaogi M, et al. (1992) High-pressure high-temperature stability ofαα-PbO_2-type TiO_2 and $MgSiO_3$ majorite: Calorimetric and *in situ* X-ray diffraction studies. *High-Pressure Research: Application to Earth and Planetary Sciences*, eds Syono Y, Manghnani MH (American Geophysical Union, Washington, DC), pp 447–455.
26. Olsen JS, Gerward L, Jiang JZ (1999) On the rutile/a-PbO_2-type phase boundary of TiO_2. *J Phys Chem Solids* 60:229–233.
27. Ono S, Tange Y, Katayama I, Kikegawa T (2004) Equations of state of $ZrSiO_4$ phases in the upper mantle. *Am Mineral* 89:185–188.
28. Andrault D, Bolfan-Casanova N (1999) High-pressure phase transformations in the $MgFe_2O_4$ and Fe_2O_3-$MgSiO_3$ systems. *Phys Chem Miner* 28:211–217.
29. Fei Y, Frost DJ, Mao HK, Prewitt CT, Häusermann D (1999) In situ structure determination of the high-pressure phase of Fe_3O_4. *Am Mineral* 84:203–206.
30. Yoo CS, Sengupta A, Kim M (2011) Carbon dioxide carbonates in the earth's mantle: Implications to the deep carbon cycle. *Angew Chem Int Ed Engl* 50:11219–11222.
31. Zuilen MA, et al. (2003) Graphite and carbonates in the 3.8 Ga old Isua Supracrustal Belt, southern West Greenland. *Precambrian Res* 126:331–348.
32. Boulard E, et al. (2012) Experimental investigation of the stability of Fe-rich carbonates in the lower mantle. *J Geophys Res: Solid Earth* 117:B02208.
33. Cerantola V, et al. (2017) Stability of iron-bearing carbonates in the deep Earth's interior. *Nat Commun* 8:15960.
34. Kelemen PB, Manning CE (2015) Reevaluating carbon fluxes in subduction zones, what goes down, mostly comes up. *Proc Natl Acad Sci USA* 112:E3997–E4006.
35. Rohrbach A, Schmidt MW (2011) Redox freezing and melting in the Earth's deep mantle resulting from carbon-iron redox coupling. *Nature* 472:209–212.
36. Jacob DE, Piazolo S, Schreiber A, Trimby P (2016) Redox-freezing and nucleation of diamond via magnetite formation in the Earth's mantle. *Nat Commun* 7:11891.
37. Ohmoto H, Watanabe Y, Kumazawa K (2004) Evidence from massive siderite beds for a CO_2-rich atmosphere before approximately 1.8 billion years ago. *Nature* 429: 395–399.
38. Palot M, et al. (2016) Evidence for H_2O-bearing fluids in the lower mantle from diamond inclusion. *Lithos* 265:237–243.
39. Wirth R, Dobrzhinetskaya L, Harte B, Schreiber A, Green HW (2014) High-Fe (Mg,Fe)O inclusion in diamond apparently from the lowermost mantle. *Earth Planet Sci Lett* 404:365–375.